THE UNIVERSITY OF
WARWICK

Original citation:
Arakawa, T., Kobayashi-Yurugi, T., Alguel, Y., Iwanari, H., Hatae, H., Iwata, M., Abe, Y., Hino, T., Ikeda-Suno, C., Kuma, H., Kang, D., Murata, T., Hamakubo, T., Cameron, A., Kobayashi, T., Hamasaki, N. and Iwata, S.. (2015) Crystal structure of the anion exchanger domain of human erythrocyte band 3. Science, 350 (6261). pp. 680-684.

Permanent WRAP url:
http://wrap.warwick.ac.uk/74238

Copyright and reuse:
The Warwick Research Archive Portal (WRAP) makes this work by researchers of the University of Warwick available open access under the following conditions. Copyright © and all moral rights to the version of the paper presented here belong to the individual author(s) and/or other copyright owners. To the extent reasonable and practicable the material made available in WRAP has been checked for eligibility before being made available.

Copies of full items can be used for personal research or study, educational, or not-for profit purposes without prior permission or charge. Provided that the authors, title and full bibliographic details are credited, a hyperlink and/or URL is given for the original metadata page and the content is not changed in any way.

Publisher's statement:
"This is the author's version of the work. It is posted here by permission of the AAAS for personal use, not for redistribution. The definitive version was published in Science on Volume 350 Number 6261 (2015) DOI: 10.1126/science.aaa4335."

A note on versions:
The version presented here may differ from the published version or, version of record, if you wish to cite this item you are advised to consult the publisher's version. Please see the 'permanent WRAP url' above for details on accessing the published version and note that access may require a subscription. For more information, please contact the WRAP Team at: publications@warwick.ac.uk

warwickpublicationswrap
highlight your research

http://wrap.warwick.ac.uk

Crystal structure of the anion exchanger domain of human erythrocyte Band 3

Takatoshi Arakawa[1, 2, 3*], Takami Kobayashi-Yugiri[1, 3*], Yilmaz Alguel[4, 5, 6]*, Hiroko Iwanari[7*], Hinako Hatae[8], Momi Iwata[4, 5], Yoshito Abe[9], Tomoya Hino[1, 3], Chiyo Ikeda-Suno[1, 2, 3], Hiroyuki Kuma[8], Dongchon Kang[10], Takeshi Murata[1, 3, 11], Takao Hamakubo[7], Alexander D. Cameron[1, 4, 5, 6, 12 ‡], Takuya Kobayashi[1, 2, 3, 13 ‡], Naotaka Hamasaki[8 ‡] and So Iwata[1, 2, 3, 4, 5, 6, 13 ‡]

1, Japan Science and Technology Agency, ERATO Human Receptor Crystallography Project, Konoe-cho, Yoshida, Sakyo-ku, Kyoto 606-8501, Japan

2, JST, Research Acceleration Program, Membrane Protein, Crystallography Project, Konoe-cho, Yoshida, Sakyo-ku, Kyoto 606-8501, Japan

3, Department of Medical Chemistry and Cell Biology, Kyoto University Faculty of Medicine, Konoe-cho, Yoshida, Sakyo-ku, Kyoto 606-8501, Japan

4, Division of Molecular Biosciences, Membrane Protein Crystallography group, Imperial College London, London SW7 2AZ, UK

5, Membrane Protein Laboratory, Diamond Light Source, Harwell Science and Innovation Campus, Didcot, Chilton, Oxfordshire OX11 0DE, U.K.

6, Research Complex at Harwell Rutherford, Appleton Laboratory, Harwell Oxford, Didcot, Oxfordshire OX110FA, U.K.

7, Department of Quantitative Biology and Medicine, Research Center for Advanced Science and Technology, The University of Tokyo, 4-6-1 Komaba, Meguro-ku, Tokyo 153-8904, Japan

8, Faculty of Pharmaceutical Sciences, Nagasaki International University, 2825-7 Huis Ten Bosch-cho, Sasebo, Nagasaki 859-3298, Japan

9, Department of Protein Structure, Function and Design, Graduate School of Pharmaceutical Sciences, Kyushu University, 3-1-1 Maidashi, Higashi-ku, Fukuoka 812-8582, Japan

10, Department of Clinical Chemistry and Laboratory Medicine, Graduate School of Medical Sciences, Kyushu University, Fukuoka 812-8582, Japan

11, Department of Chemistry, Graduate School of Science, Chiba University, 1-33 Yayoi-cho, Inage, Chiba 263-8522, Japan

12, School of Life Sciences, University of Warwick, Gibbet Hill Road, Coventry, CV4 7AL, U.K.

13, Platform for Drug Discovery, Informatics, and Structural Life Science, Konoe-cho, Yoshida, Sakyo-ku, Kyoto 606-8501, Japan

**These authors contributed equally to this work.*

‡To whom correspondence should be addressed. E-mails: a.cameron@warwick.ac.uk; naotaka.hamasaki@city.sasebo.lg.jp; mailto:t-coba@mfour.med.kyoto-u.ac.jp; mailto:s.iwata@imperial.ac.uk

One sentence summary: Structure of erythrocyte Band 3 reveals mutation locations leading to red cell diseases.

Abstract

Anion Exchanger 1 (AE1, SLC4A1), also known as Band 3 plays a key role in the removal of carbon dioxide from tissues by facilitating the exchange of chloride and bicarbonate across the plasma membrane of erythrocytes. An isoform of AE1 is also present in the kidney. Specific mutations in human AE1 cause several types of hereditary hemolytic anemias and/or distal renal tubular acidosis. Here, we report the crystal structure of the Band 3 anion exchanger domain ($AE1_{CTD}$) at 3.5 Å. The structure is locked in an outward-facing open conformation by an inhibitor, H_2DIDS. Comparing this structure to a substrate bound structure of the UraA uracil transporter in an inward-facing conformation allowed us to identify the anion-binding position in the $AE1_{CTD}$ and to propose a possible transport mechanism revealing why selected mutations lead to disease.

Efficient delivery of oxygen to tissues and removal of carbon dioxide in blood is fundamental for respiration. The red blood cells or erythrocytes provide the principal route to achieve this. Anion exchanger 1 (AE1), also known as Band 3 or SLC4A1 predominates in the erythrocyte ghost membrane and constitutes 30% of its protein *(1).* It plays a major role in gas transport by converting the CO_2 generated to the more soluble bicarbonate form (HCO_3^-), increasing the CO_2 bearing capacity of the blood. Carbon dioxide rising from metabolic processes in the tissues diffuses into the red blood cells. Here it reacts with water in a reversible process catalysed by carbonic anhydrase II to form HCO_3^- and protons *(2)*. As the bicarbonate concentration in the erythrocyte increases, the anions are transported by AE1 out into the blood plasma in an electroneutral exchange for chloride ions. With approximately 10^6 AE1 molecules per cell *(1)* and each single protein transporting 4-5 x 10^4 ions per second *(3,4),* transport is extremely fast and approximately 90% of CO_2 is taken from the tissues to the lungs as bicarbonate. Within the erythrocyte the net result is the accumulation of protons from the hydration of CO_2. Due to the Bohr effect, the low pH causes hemoglobin to release oxygen, which can then diffuse into the tissues. When the blood reaches the lungs, the process is reversed and CO_2 is exhaled.

Erythrocyte AE1 is the most abundant and widely studied anion exchanger but AE1 and its close homologues AE2 and AE3 are found in diverse tissues *(5,6),* playing important roles in the regulation of intracellular pH, cell volume and membrane potential through HCO_3^-/Cl^- exchange. AE1 is highly expressed as an N-terminally truncated form in kidney, where it is instrumental in the reabsorption of bicarbonate *(7)*. Many morphological and anemic disorders to the erythrocytes and distal renal tubular acidosis in kidney are caused by inherited mutations in AE1 *(8)*.

Human erythrocyte AE1 is a 110kDa glycoprotein. It is built from two domains (*9*), a cytosolic N-terminal domain (residues 1-360) and an integral membrane domain (residues 361-911). Anion exchange is catalyzed by the C-terminal domain *(10-12).* However, only the crystal structure of the cytosolic N-terminal domain *(13),* important as an anchoring point for other proteins including the scaffolding protein ankyrin (*14, 15*) and deoxy-hemoglobin, has been determined *(16,17).* A wealth of biochemical experiments, including cysteine scanning mutagenesis *(18-23)* and N-glycan insertion mutagenesis *(24,25),* have been used to derive topology models of AE1. The only 3-dimensional structural information available to date for the transmembrane domain is from electron microscopy *(26,27)* with the best maps at a resolution of 7.5Å calculated from 2-dimensional crystals *(28).* As such, the membrane topology, substrate recognition and the anion-transport mechanism of this fundamental protein remain unclear and diverse models have been proposed *(28-31).* Here we report the crystal structure at 3.5Å resolution of the membrane domain of human AE1 locked in an outward-facing open conformation by a covalently bound H_2DIDS-inhibitor, in complex with a Fab fragment from a monoclonal antibody.

The C-terminal, anion exchanger domain of AE1 ($AE1_{CTD}$), with the N-terminus cleaved by trypsin, was purified directly from white ghost membranes of human erythrocytes and was treated with H_2DIDS (4,4-diisothiocyanatodihydro-stilbene-2,2-disulfonic acid), a disulfonic stilbene derivative that irreversibly inhibits anion exchangers by covalently binding to the protein and blocking the transport cycle *(32,33)*. Two steps were required to obtain well diffracting crystals. Firstly the transporter was deglycosylated with N-glycosidase F. Secondly, the protein was cocrystallised with a monoclonal antibody that binds tightly to a conformational epitope of $AE1_{CTD}$. This was selected from a panel of antibodies raised by the inoculation of mice with budded

baculovirus displaying $AE1_{CTD}$ *(34).* The structure was solved using MIRAS in combination with non-crystallographic symmetry averaging and refined at a resolution of 3.5Å to an R-factor of 27.4% and R-free of 29.0% (Tables S1 and S2) *(32)*. The final model contains all residues from 381 to 887 apart from three loop regions (553-567, 640-649, 742-753). The asymmetric unit of the crystal contains two dimers of $AE1_{CTD}$ with one Fab fragment bound on the outer side of each protomer (Figs. S1 and S2).

Each protomer comprises 14 transmembrane (TM) segments (Fig. 1) and has dimensions of approximately 60 x 60 x 50 Å. The lengths of the individual TMs vary from 18 to 42 Å. Like many other secondary transporters, the structure is built from two repeats inverted in the plane of the membrane (Fig. S3). In $AE1_{CTD}$, the repeat is made of 7 TMs with the third TM of each repeat only partially spanning the membrane before the helical structure unravels. Though it is difficult to superimpose all TMs from the inverted repeat as a unit, treating it as a two-component module TM1-4 can be superimposed on TM 8-11 (root-mean-square deviation (r.m.s.d.) of 2.1Å for 62 out of 103 Cα atoms; see methods) and TM 5-7 onto TM 12-14 (r.m.s.d. of 2.1Å for 53 out of 100 Cα atoms) (Fig. S3B).

The inverted repeat units intertwine to form two structural domains separated by a cleft on the extracellular side of the protein (Fig. 1A). We define these structural domains as the Core (TMs1-4 and 8-11) and the Gate (TMs 5-7 and 12-14), domains following the convention of UraA *(35,36).* Within the core domain, the N-termini of the two half-helices (TMs 3 and 10) face one another at a distance of ~10 Å giving the appearance of a continuous helix (Figs. 2A, B and S2B).

The overall fold of AE1 is very similar to the structure of the uracil transporter UraA *(35)* although they have only 12% sequence identity as aligned using the structures (Fig. S4). Structural similarity was previously suggested based on threading

combined with mutagenesis experiments *(29).* UraA is also made of two 7 TM repeat units forming two domains. As shown in Figure 2, the Core domains of $AE1_{CTD}$ and UraA are similar and can be superposed with an r.m.s.d. of 1.8 Å for 145 of 268 Cα atoms (1.9 Å for 131 out of 190 Cα atoms if only the TM segments are considered; Fig. S5). The Gate domains of the two proteins also have the same topology but it is more difficult to superpose these domains (r.m.s.d. of 2.0 Å for only 55 out of 166 Cα atoms) (Fig. 2, C and D and Fig. S5). This is, in part, because the relative positions of the three pairs of helices (TMs 5 and 12, TMs 6 and 7 and TMs 13 and 14) are different between AE1 and UraA. As the gate domains are directly involved in substrate binding, as discussed below, the structural variation could reflect the different substrates of the two proteins.

$AE1_{CTD}$ is a physiological dimer (*37*) but dimerization is not necessary for transport *(38,39)*. The dimer in the crystal consists of two $AE1_{CTD}$ monomers with 1092 $Å^2$ of surface area buried at the interface (*32*). Monomers are related by a 2-fold axis parallel to the membrane normal, consistent with dimer formation in the erythrocyte membrane (Fig. 1B). There is no obvious difference between the two dimers seen in the crystal at the current resolution. The interaction between subunits is formed exclusively through residues on the Gate domains including TMs 5, 6 and 7 (Fig. 1B).

The Fab fragments bind solely to the Core domain of each $AE1_{CTD}$ (Figs. S1 and S2). The interactions between $AE1_{CTD}$ and the Fab are identical for the four molecules of the asymmetric unit. The predominant interactions are between the heavy chain of the Fab and the C-terminal end of TM 3, the following loop and the loop before TM 8 (Fig. S1). The light chain of the Fab interacts with the end of TM 1 and the following loop.

H_2DIDS covalently crosslinks Lys539 and Lys851 *(40)* and, in the electron density maps, there is non-protein density between them consistent with the inhibitor (Fig. S6). However, part of the H_2DIDS density is ill-defined and it is possible that either the link

may have been damaged by radiation or the cross-linking may not have been carried out to completion (Fig. S6A,B). The H_2DIDS molecule spans TMs 5 and 13 of the Gate domain (Fig. 2A) at the entrance of a large cavity 15 Å wide, 7 Å long and 11 Å deep on the extracellular side of the protein between the Core and Gate domains (Figs. 3A, S6, S7 and S8). The cavity is formed by TMs 1, 3, 5, 13 and 14 and has predominantly hydrophobic walls with polar residues near the entrance and at the bottom.

Mutagenesis studies of mouse AE1 demonstrate that the protein is still capable of Cl^- self-exchange when the lysine residues interacting with H_2DIDS are mutated *(41)* suggesting that the inhibitor does not bind in the same place as the substrate. Under the H_2DIDS molecule the cavity opens out slightly (18 Å) where the N-termini of TMs 3 and 10 meet (Fig. 3). This region has been suggested as a cation selectivity filter *(23).* In UraA, uracil binds in the space between the positive dipoles TMs 3 and 10. The uracil interacts with two glutamate residues, one on TM8 (Glu241) and the other on TM 10 (Glu290) (Fig. 3B) (*35*). In $AE1_{CTD}$, Glu681 and the positively charged Arg730 take the positions of these two glutamates on TMs 8 and 10, respectively (Fig. 3B). Both of these residues are conserved in AE1, and anion exchange is lost if either is mutated *(19, 42-44).* Though there is no apparent density for a substrate and substrate binding could be blocked by bound H_2DIDS, a bicarbonate ion can be placed between the positive dipoles of TMs 3 and 10. The negatively charged bicarbonate could interact with the positively charged Arg730, and could hydrogen bond to Glu681. The anions may also interact directly with the amide protons at the N-termini of TMs 3 and 10 (Fig. 3B). Consistent with anion binding in this space, mutagenesis studies indicate that only a conservative mutation to a threonine *(30)* or cysteine *(29)* is tolerated at Ser465 at the N-terminus of TM3. Mutation to the larger isoleucine *(29),* asparagine or aspartic acid *(30)* abolishes transport. The arrangement of an anion between the positively charged dipoles of half-

helices (TMs 3 and 10 in AE1) with a negatively charged residue nearby (Glu681 in AE1) is similar to the selectivity filter of the CLC chloride transporter although the topology of the two proteins is completely different (Fig. S9) *(45)*.

AE1 exhibits modes of transport other than the physiological 1:1 exchange of bicarbonate and chloride ions. It can also conduct anions *(46)* or cotransport protons to drive the uptake of divalent sulfate *(47)* or chloride ions *(48)*. These ions can easily be accommodated in the basic cavity (Figs. S7 and S8). Glu681 on the translocation pathway is a potential proton acceptor during H^+/SO_4^{2-} cotransport as modification to an alcohol (Glu681OH) or mutation to a glutamine leads to a highly proton independent SO_4^{2-}/Cl^- exchange, and electroneutral SO_4^{2-}/ SO_4^{2-} exchange *(42, 49-50).*

Specific mutations in the $AE1_{CTD}$ domain (Fig. S10), are related to red cell diseases such as spherocytosis *(51),* stomatocytosis *(52)* and southeast asian ovalocytosis (SAO)*(53).* Some of these mutations, particularly those leading to spherocytosis, cause misfolding of the protein whereas others exhibit abnormal transport kinetics. Some of the mutations in the transport domain are listed in Table S3 and shown in Figs. 4 and S11, S12. An increase in membrane permeability to monovalent cations caused by mutations in AE1 has been seen in a number of human pedigrees with dominantly inherited hemolytic anemia *(22, 44, 52).* These mutations mostly occur on the cytoplasmic half of the Core domain (Fig. 4). They include mutation of Arg730, the putative bicarbonate-binding residue, to Cys as well as two other mutations on the half-helix TM10 (Ser731 to Pro, His734 to Arg). The deletion of residues 400 to 408 leading to SAO also causes a cation leak in intact red cells *(54).* These residues reside at the N-terminus of TM 1 where it interacts with TM 7 of the Gate domain (Figs. 4 and S12) and would presumably alter the structure of the Core domain as well as the interaction between $AE1_{CTD}$ and the N-terminal cytoplasmic domain. It is

interesting that this deletion may confer protection against cerebral malaria *(54)*. Fewer mutations have been reported in the Gate domain.

The structure of $AE1_{CTD}$ reported here is in an outward-facing conformation (Fig. 1 and 3). $AE1_{CTD}$ is reported to undergo large conformational changes during transport in line with the alternating access mechanism *(55, 56)*. By comparing the structures of outward-facing $AE1_{CTD}$ and inward-facing UraA with a bound substrate *(35)*, we can gain some insight into the mechanism (Figs. 3A and S13).

The Core domain of these two proteins, including the uracil binding site in UraA, is very similar (Figs. 3B and S5). The major difference between the two structures is seen in the relative positions of the Gate and Core domains (Fig. 2, C and D and Fig. S5). The rotation of one domain against another as the transporter moves from outward to inward facing, as seen in Fig. S5, is very similar to the predominant movements seen for other families of transporters including the LeuT family transporters to which there is some structural similarity (Fig. S14) *(36, 57-61)*. Fig. S13 shows a possible transport mechanism of AE1. Starting from an outward-facing open conformation of the protein, chloride at a high concentration in plasma, binds to the anion-binding site. This causes some local conformational changes of the Core domain enabling this domain to rotate against the Gate domain to form the inward-facing structure. At this point chloride diffuses out and is replaced by bicarbonate to reverse the process. This is consistent with various results in kinetic studies indicating that chloride and bicarbonate ions share the same binding site *(4)*. The structure of the human $AE1_{CTD}$ and the proposed transport mechanism provides a scaffold through which to understand the many mutations in the protein that lead to diseases.

Supplementary Materials

www.sciencemag.org
Materials and Methods
Figs. S1 to S15
References (63 - 85)
Tables S1 to S3

References and Notes

1. G. Fairbanks, T. L. Steck, D. F. Wallach, Electrophoretic analysis of the major polypeptides of the human erythrocyte membrane. *Biochemistry* **10**, 2606-2617 (1971).

2. J. W. Vince, R. A. Reithmeier, Identification of the carbonic anhydrase II binding site in the Cl(-)/HCO(3)(-) anion exchanger AE1. *Biochemistry* **39**, 5527-5533 (2000).

3. J. Brahm, Temperature-dependent changes of chloride transport kinetics in human red cells. *J. Gen. Physiol.* **70**, 283-306 (1977).

4. H. Passow, Molecular aspects of band 3 protein-mediated anion transport across the red blood cell membrane. *Rev. Physiol. Biochem. Pharmacol.* **103**, 61-203 (1986).

5. S. L. Alper, R. R. Kopito, S. M. Libresco, H. F. Lodish, Cloning and characterization of a murine band 3-related cDNA from kidney and from a lymphoid cell line. *J. Biol. Chem.* **263**, 17092-17099 (1988).

6. R. R. Kopito, B. S. Lee, D. M. Simmons, A. E. Lindsey, C. W. Morgans, K. Schneider, Regulation of intracellular pH by a neuronal homolog of the erythrocyte anion exchanger. *Cell* **59**, 927-937 (1989).

7. F. C. Brosius, 3rd, S. L. Alper, A. M. Garcia, H. F. Lodish, The major kidney band 3 gene transcript predicts an amino-terminal truncated band 3 polypeptide. *J. Biol. Chem.* **264**, 7784-7787 (1989).

8. S. L. Alper, Molecular physiology and genetics of Na+-independent SLC4 anion exchangers. *J. Exp. Biol.* **212**, 1672-1683 (2009).

9. R. R. Kopito, H. F. Lodish, Primary structure and transmembrane orientation of the murine anion exchange protein. *Nature* **316**, 234-238 (1985).

10. S. Lepke, H. Passow, Effect of incorporated trypsin on anion exchange and membrane protein in human red blood cell ghosts. *Biochim. Biophys. Acta* **455**, 353-370 (1976).

11. S. Grinstein, S. Ship, A. Rothstein, Anion transport in relation to proteolytic dissection of band 3 protein. *Biochim. Biophys. Acta* **507**, 294-304 (1978).

12. S. Lepke, A. Becker, H. Passow, Mediation of inorganic anion transport by the hydrophobic domain of mouse erythroid band 3 protein expressed in oocytes of Xenopus laevis. *Biochim. Biophys. Acta* **1106**, 13-16 (1992).

13. D. Zhang, A. Kiyatkin, J. T. Bolin, P. S. Low, Crystallographic structure and functional interpretation of the cytoplasmic domain of erythrocyte membrane band 3. *Blood* **96**, 2925-2933 (2000).

14. J. L. Grey, G. C. Kodippili, K. Simon, P. S. Low, Identification of Contact Sites between Ankyrin and Band 3 in the Human Erythrocyte Membrane. *Biochemistry* **51**, 6838-6846 (2012).

15. L. Davis, S. E. Lux, V. Bennett, Mapping the ankyrin-binding site of the human erythrocyte anion exchanger. *J. Biol. Chem.* **264**, 9665-9672 (1989).

16. M. J. Tanner, Band 3 anion exchanger and its involvement in erythrocyte and kidney disorders. *Curr. Opin. Hematol.* **9**, 133-139 (2002).

17. J. A. Walder, R. Chatterjee, T. L. Steck, P. S. Low, G. F. Musso, E. T. Kaiser, P. H. Rogers, A. Arnone, The interaction of hemoglobin with the cytoplasmic domain of band 3 of the human erythrocyte membrane. *J. Biol. Chem.* **259**, 10238-10246 (1984).

18. J. Fujinaga, X. B. Tang, J. R. Casey, Topology of the membrane domain of human erythrocyte anion exchange protein, AE1. *J. Biol. Chem.* **274**, 6626-6633 (1999).

19. X. B. Tang, J. Fujinaga, R. Kopito, J. R. Casey, Topology of the region surrounding Glu681 of human AE1 protein, the erythrocyte anion exchanger. *J. Biol. Chem.* **273**, 22545-22553 (1998).

20. A. M. Taylor, Q. Zhu, J. R. Casey, Cysteine-directed cross-linking localizes regions of the human erythrocyte anion-exchange protein (AE1) relative to the dimeric interface. *Biochem. J.* **359**, 661-668 (2001).

21. Q. Zhu, D. W. Lee, J. R. Casey, Novel topology in C-terminal region of the human plasma membrane anion exchanger, AE1. *J. Biol. Chem.* **278**, 3112-3120 (2003).

22. D. Barneaud-Rocca, B. Pellissier, F. Borgese, H. Guizouarn, Band 3 missense mutations and stomatocytosis: insight into the molecular mechanism responsible for monovalent cation leak. *Int. J. Cell Biol*. **2011**, 136802 (2011).

23. Q. Zhu, J. R. Casey, The substrate anion selectivity filter in the human erythrocyte Cl-/HCO3- exchange protein, AE1. *J. Biol. Chem.* **279**, 23565-23573 (2004).

24. J. C. Cheung, R. A. Reithmeier, Membrane integration and topology of the first transmembrane segment in normal and Southeast Asian ovalocytosis human erythrocyte anion exchanger 1. *Mol. Membr. Biol.* **22**, 203-214 (2005).

25. M. Popov, J. Li, R. A. Reithmeier, Transmembrane folding of the human erythrocyte anion exchanger (AE1, Band 3) determined by scanning and insertional N-glycosylation mutagenesis. *Biochem. J.* **339**, 269-279 (1999).

26. D. N. Wang, W. Kühlbrandt, V. E. Sarabia, R. A. Reithmeier, Two-dimensional structure of the membrane domain of human band 3, the anion transport protein of the erythrocyte membrane. *EMBO J.* **12**, 2233-2239 (1993).

27. D. N. Wang, V. E. Sarabia, R. A. Reithmeier, W. Kühlbrandt, Three-dimensional map of the dimeric membrane domain of the human erythrocyte anion exchanger, Band 3. *EMBO J.* **13**, 3230-3235 (1994).

28. T. Yamaguchi, Y. Ikeda, Y. Abe, H. Kuma, D. Kang *et al.*, Structure of the membrane domain of human erythrocyte anion exchanger 1 revealed by electron crystallography. *J. Mol. Biol*. **397**, 179-189 (2010).

29. D. Barneaud-Rocca, C. Etchebest, H. Guizouarn, Structural model of the anion exchanger 1 (SLC4A1) and identification of transmembrane segments forming the transport site. *J. Biol. Chem.* **288**, 26372-26384 (2013).

30. P. Bonar, H. P. Schneider, H. M. Becker, J. W. Deitmer, J. R. Casey, Three-dimensional model for the human Cl-/HCO3- exchanger, AE1, by homology to the E. coli ClC protein. *J. Mol. Biol.* **425**, 2591-2608 (2013).

31. T. Hirai, N. Hamasaki, T. Yamaguchi, Y. Ikeda, Topology models of anion exchanger 1 that incorporate the anti-parallel V-shaped motifs found in the EM structure. *Biochem. Cell Biol.* **89**, 148-156 (2011).

32. Materials and methods are available as supplementary information on Science Online.

33. Y. Shami, A. Rothstein, P. A. Knauf, Identification of the Cl- transport site of human red blood cells by a kinetic analysis of the inhibitory effects of a chemical probe. *Biochim. Biophys. Acta* **508**, 357-363 (1978).

34. R. Saitoh, T. Ohtomo, Y. Yamada, N. Kamada, J. Nezu *et al.*, Viral envelope protein gp64 transgenic mouse facilitates the generation of monoclonal antibodies against exogenous membrane proteins displayed on baculovirus. *J. Immuno. Methods* **322**, 104-117 (2007).

35. F. Lu, S. Li, Y. Jiang, J. Jiang, H. Fan *et al.* Structure and mechanism of the uracil transporter UraA. *Nature* **472**, 243-246 (2011).

36. A. Vastermark, M. H. Saier, Jr., Evolutionary relationship between 5+5 and 7+7 inverted repeat folds within the amino acid-polyamine-organocation superfamily. *Proteins* **82**, 336-346 (2014).

37. J. R. Casey, R. A. Reithmeier, Analysis of the oligomeric state of Band 3, the anion transport protein of the human erythrocyte membrane, by size exclusion high performance liquid chromatography. Oligomeric stability and origin of heterogeneity. *J. Biol. Chem.* **266**, 15726-15737 (1991).

38. N. K. Dahl, L. Jiang, M. N. Chernova, A. K. Stuart-Tilley, B. E. Shmukler, S. L. Alper, Deficient HCO3- transport in an AE1 mutant with normal Cl- transport can be

rescued by carbonic anhydrase II presented on an adjacent AE1 protomer. *J. Biol. Chem.* **278**, 44949-44958 (2003).

39. S. Lindenthal, D. Schubert, Monomeric erythrocyte band 3 protein transports anions. *Proc. Natl. Acad. Sci. U S A* **88**, 6540-6544 (1991).

40. K. Okubo, D. Kang, N. Hamasaki, M. L. Jennings, Red blood cell band 3. Lysine 539 and lysine 851 react with the same H2DIDS (4,4'-diisothiocyanodihydrostilbene-2,2'-disulfonic acid) molecule. *J. Biol. Chem.* **269**, 1918-1926 (1994).

41. P. G. Wood, H. Müller, M. Sovak, H. Passow, Role of Lys 558 and Lys 869 in substrate and inhibitor binding to the murine band 3 protein: a study of the effects of site-directed mutagenesis of the band 3 protein expressed in the oocytes of Xenopus laevis. *J. Membr. Biol.* **127**, 139-148 (1992).

42. M. N. Chernova, L. Jiang, M. Crest, M. Hand, D. H. Vandorpe *et al.*, Electrogenic sulfate/chloride exchange in Xenopus oocytes mediated by murine AE1 E699Q. *J Gen. Physiol*.**109**, 345-360 (1997).

43. D. Karbach, M. Staub, P. G. Wood, H. Passow, Effect of site-directed mutagenesis of the arginine residues 509 and 748 on mouse band 3 protein-mediated anion transport. *Biochim. Biophys. Acta* **1371**, 114-122 (1998).

44. A. K. Stewart, P. S. Kedar, B. E. Shmukler, D. H. Vandorpe, A. Hsu *et al.*, Functional characterization and modified rescue of novel AE1 mutation R730C associated with overhydrated cation leak stomatocytosis. *Am. J. Physiol. Cell Physiol.* **300**, C1034-1046 (2011).

45. R. Dutzler, E. B. Campbell, M. Cadene, B. T. Chait, R. MacKinnon, X-ray structure of a ClC chloride channel at 3.0 A reveals the molecular basis of anion selectivity. *Nature* **415**, 287-294 (2002).

46. P. A. Knauf, G. F. Fuhrmann, S. Rothstein, A. Rothstein, The relationship between anion exchange and net anion flow across the human red blood cell membrane. *J. Gen. Physiol.* **69**, 363-386 (1977).

47. M. L. Jennings, Proton fluxes associated with erythrocyte membrane anion exchange. *J. Membr. Biol.* **28**, 187-205 (1976).

48. M. L. Jennings, Characteristics of CO2-independent pH equilibration in human red blood cells. *J. Membr. Biol.* **40**, 365-391 (1978).

49. M. L. Jennings, J. S. Smith, Anion-proton cotransport through the human red blood cell band 3 protein. Role of glutamate 681. *J. Biol. Chem.* **267**, 13964-13971 (1992).

50. X. B. Tang, M. Kovacs, D. Sterling, J. R. Casey, Identification of residues lining the translocation pore of human AE1, plasma membrane anion exchange protein. *J. Biol. Chem.* **274**, 3557-3564 (1999).

51. P. Jarolim, H. L. Rubin, V. Brabec, L. Chrobak, A. S. Zolotarev *et al.*, Mutations of conserved arginines in the membrane domain of erythroid band 3 lead to a decrease in membrane-associated band 3 and to the phenotype of hereditary spherocytosis. *Blood* **85**, 634-640 (1995).

52. L. J. Bruce, H. C. Robinson, H. Guizouarn, F. Borgese, P. Harrison *et al.*, Monovalent cation leaks in human red cells caused by single amino-acid substitutions in the transport domain of the band 3 chloride-bicarbonate exchanger, AE1. *Nat. Genet.* **37**, 1258-1263 (2005).

53. P. Jarolim, J. Palek, D. Amato, K. Hassan, P. Sapak *et al.*, Deletion in erythrocyte band 3 gene in malaria-resistant Southeast Asian ovalocytosis. *Proc. Natl. Acad. Sci. U S A* **88**, 11022-11026 (1991).

54. L. J. Bruce, S. M. Ring, K. Ridgwell, D. M. Reardon, C. A. Seymour *et al.*, South-east asian ovalocytic (SAO) erythrocytes have a cold sensitive cation leak: implications for in vitro studies on stored SAO red cells. *Biochim. Biophys. Acta* **1416**, 258-270 (1999).

55. O. Jardetzky, Simple allosteric model for membrane pumps. *Nature* **211**, 969-970 (1966).

56. W. Furuya, T. Tarshis, F. Y. Law, P. A. Knauf, Transmembrane effects of intracellular chloride on the inhibitory potency of extracellular H2DIDS. Evidence for two conformations of the transport site of the human erythrocyte anion exchange protein. *J. Gen. Physiol.* **83**, 657-681 (1984).

57. C. Lee, H. J. Kang, C. von Ballmoos, S. Newstead, P. Uzdavinys *et al.*, A two-domain elevator mechanism for sodium/proton antiport. *Nature* **501**, 573-577 (2013).

58. E. M. Quistgaard, C. Löw, P. Moberg, L. Trésaugues, P. Nordlund, Structural basis for substrate transport in the GLUT-homology family of monosaccharide transporters. *Nat. Struct. Mol. Biol.* **20**, 766-768 (2013).

59. N. Reyes, C. Ginter, O. Boudker, Transport mechanism of a bacterial homologue of glutamate transporters. *Nature* **462**, 880-885 (2009).

60. T. Shimamura, S. Weyand, O. Beckstein, N. G. Rutherford, J. M. Hadden *et al.*, Molecular Basis of Alternating Access Membrane Transport by the Sodium-Hydantoin Transporter Mhp1. *Science* **328**, 470-473 (2010).

61. X. Zhou, E. J. Levin, Y. Pan, J. G. McCoy, R. Sharma *et al.*, Structural basis of the alternating-access mechanism in a bile acid transporter. *Nature* **505**, 569-573 (2014).

62. F. Glaser, T. Pupko, I. Paz, R. E. Bell, D. Bechor-Shental *et al.*, ConSurf: identification of functional regions in proteins by surface-mapping of phylogenetic information. *Bioinformatics* **19**, 163-164 (2003).

63. N. Hamasaki, K. Okubo, H. Kuma, D. Kang, Y. Yae, Proteolytic cleavage sites of band 3 protein in alkali-treated membranes: fidelity of hydropathy prediction for band 3 protein. *J. Biochem.* **122,** 577-585 (1997).

64. T. Hino, S. Iwata, T. Murata, Generation of functional antibodies for mammalian membrane protein crystallography. *Curr. Opin. Struct. Biol* **23**, 563-568 (2013).

65. Z. Otwinowski and W. Minor, Processing of X-ray diffraction data collected in oscillation mode. *Methods Enzymol.* **276**, 307-326 (1997).

66. J. Foadi, P. Aller, Y. Alguel, A. Cameron, D. Axford *et al.*, Clustering procedures for the optimal selection of data sets from multiple crystals in macromolecular crystallography. *Acta Crystallogr. D Biol. Crystallogr.* **69**, 1617-1632 (2013).

67. A. G. Leslie, H. R. Powell, G. Winter, O. Svensson, D. Spruce *et al.*, Automation of the collection and processing of X-ray diffraction data -- a generic approach. *Acta Crystallogr. D Biol. Crystallogr.* **58**, 1924-1928 (2002).

68. Collaborative Computational Project Number 4, The CCP4 suite: programs for protein crystallography. *Acta Crystallogr. D Biol. Crystallogr.* **50**, 760-763 (1994).

69. A. J. McCoy, R. W. Grosse-Kunstleve, P. D. Adams, M. D. Winn, L. C. Storoni *et al.*, Phaser crystallographic software. *J. Appl. Crystallogr.* **40**, 658-674 (2007).

70. G. Bricogne, C. Vonrhein, C. Flensburg, M. Schiltz, W. Paciorek, Generation, representation and flow of phase information in structure determination: recent developments in and around SHARP 2.0. *Acta Crystallogr. D Biol. Crystallogr.* **59**, 2023-2030 (2003).

71. J. P. Abrahams, A. G. Leslie, Methods used in the structure determination of bovine mitochondrial F1 ATPase. *Acta Crystallogr. D Biol. Crystallogr.* **52**, 30-42 (1996).

72. G. J. Kleywegt, J. Y. Zou, M. Kjeldgaard, T. A. Jones, in *International Tables for Crystallography, Volume F. Crystallography of Biological Macromolecules,* M. G. Rossmann, E. Arnold, Eds. (Kluwer Academic Publishers, Dordrecht, 2001), chap. 21.1, pp. 497-506, 526-528.

73. T. A. Jones, M. Kjeldgaard, Electron-density map interpretation. *Methods Enzymol.* **277**, 173-208 (1997).

74. P. Emsley, K. Cowtan, Coot: model-building tools for molecular graphics. *Acta Crystallogr. D Biol. Crystallogr.* **60**, 2126-2132 (2004).

75. P. D. Adams, P. V. Afonine, G. Bunkoczi, V. B. Chen, I. W. Davis *et al.*, PHENIX: a comprehensive Python-based system for macromolecular structure solution. *Acta Crystallogr. D Biol. Crystallogr.* **66**, 213-221 (2010).

76. M. D. Winn, M. N. Isupov, G. N. Murshudov, Use of TLS parameters to model anisotropic displacements in macromolecular refinement. *Acta Crystallogr. D Biol. Crystallogr.* **57**, 122-133 (2001).

77. B. DeLaBarre, A. T. Brunger, Considerations for the refinement of low-resolution crystal structures. *Acta Crystallogr. D Biol. Crystallogr.* **62**, 923-932 (2006).

78. W. L. Delano, The PyMOL Molecular Graphics System. *DeLano Scientific, Palo Alto, CA, USA*, http://www.pymol.org (2002).

79. G. J. Kleywegt, T. A. Jones, A super position. *ESF/CCP4 Newsletter* **31**, 9-14 (1994).

80. I. W. Davis, A. Leaver-Fay, V. B. Chen, J. N. Block, G. J. Kapral *et al.*, MolProbity: all-atom contacts and structure validation for proteins and nucleic acids. *Nucleic Acids Res.* **35**, W375-383 (2007).

81. A. K. Stewart, P. S. Kedar, B. E. Shmukler, D. H. Vandorpe, A. Hsu *et al.*, Functional characterization and modified rescue of novel AE1 mutation R730C associated with overhydrated cation leak stomatocytosis. *Am. J. Physiol. Cell Physiol.* **300**, C1034-1046 (2011).

82. A. K. Stewart, D. H. Vandorpe, J. F. Heneghan, F. Chebib, K. Stolpe *et al.*, The GPA-dependent, spherostomatocytosis mutant AE1 E758K induces GPA-independent, endogenous cation transport in amphibian oocytes. *Am. J. Physiol. Cell Physiol.* **298**, C283-297 (2010).

83. J. C. Ellory, H. Guizouarn, F. Borgese, L. J. Bruce, R. J. Wilkins *et al.*, Review. Leaky Cl--HCO3- exchangers: cation fluxes via modified AE1. *Philos. Trans. R. Soc. Lond. B Biol. Sci.* **364**, 189-194 (2009).

84 L. J. Bruce, M. M. Kay, C. Lawrence, M. J. Tanner, Band 3 HT, a human red-cell variant associated with acanthocytosis and increased anion transport, carries the mutation Pro-868-->Leu in the membrane domain of band 3. *Biochem. J.* **293**, 317-320 (1993).

85 J. M. Salhany, L. M. Schopfer, M. M. Kay, D. N. Gamble, C. Lawrence, Differential sensitivity of stilbenedisulfonates in their reaction with band 3 HT (Pro-868-->Leu). *Proc. Natl. Acad. Sci. U S A* **92**, 11844-11848 (1995).

Acknowledgments We thank the beamline scientists at Diamond Light Source, ESRF and SPring 8 for help with data collection, Dr. Lesley Bruce at the Bristol Institute for Transfusion Sciences, NHS Blood and Transplant and Dr. Ash Toye at the University of Bristol for useful discussion. Dr. Simone Weyand contributed to the refinement of the Fab fragment and Dr. Ryoji Suno at Kyoto University to the preparation of the figures. The project was funded by the Biotechnology and Biological Sciences Research Council (BB/G023425/1 and BB/D019516/1 to S.I.), the ERATO Human Receptor Crystallography Project from the Japan Science and Technology Agency (to S.I.), the Targeted Proteins Research Program of MEXT (to S.I.), a Grant-in-Aid for Scientific Research (B) (20370035, 23370049, to T.K.), Platform for Drug Discovery, Informatics, and Structural Life Science from the Ministry of Education, Culture, Sports, Science and Technology, Japan (to T.K. and S.I.) and the EU (European Drug Initiative for Channels and Transporters, EDICT grant 201924 to S.I. and AC). The authors are grateful for the use of the Membrane Protein Laboratory funded by the Wellcome Trust (WT089809) at the Diamond Light Source Limited. The authors declare no competing interests. The project was conceived by SI, DK and NH. HH, HK and NH purified the $AE1_{CTD}$ protein. HI and THamakubo raised the antibody using the $AE1_{CTD}$ expressing baculovirus as an antigen. TA, THino, CI-S and TM screened the antibody. TK-Y, TK, TA, YAbe and MI crystallized the $AE1_{CTD}$ protein. TK, YA, AC and SI collected diffraction data. The structure was solved and refined by YA and AC. The manuscript was written by TK, AC, YA and SI. The coordinates and structure factors have been deposited with the Protein Data Bank (4YZF: Band 3 with Fab4201, 5a16: Fab4201).

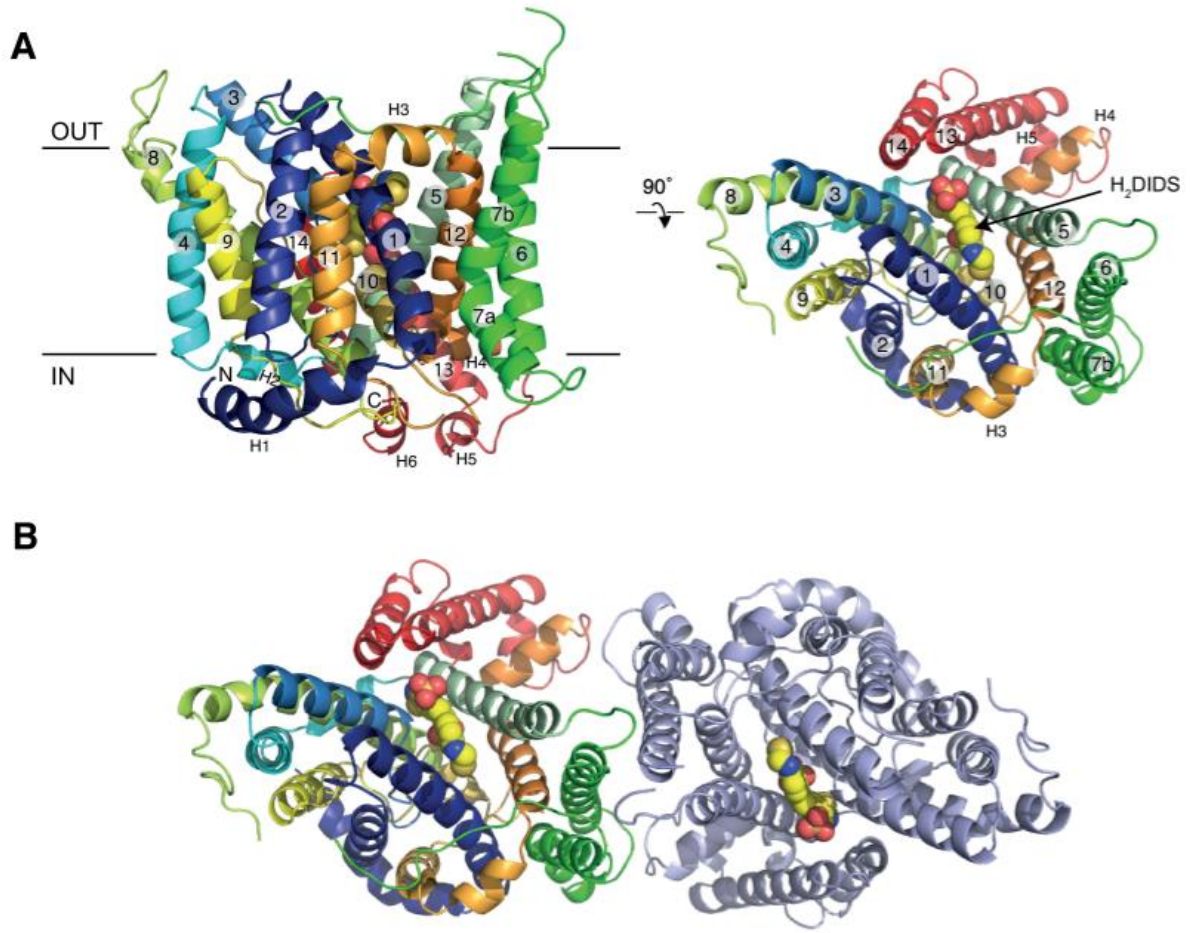

Fig. 1. Structure of AE1$_{CTD}$ in an outward-facing conformation. **(A)** View of the structure in the plane of the membrane (left) and from the extracellular side of the membrane (right). The cartoon representation of the structure has been colored from blue at the N-terminus to red at the C-terminus. The H_2DIDS is depicted by spheres (C: yellow, S: dark yellow, O: red and N: blue). Six short helices on the membrane surface are shown as H1 – H6. **(B)** Structure of the dimer viewed from the extracellular side. The color coding of the left monomer is the same as in (A). The right monomer is shown in grey.

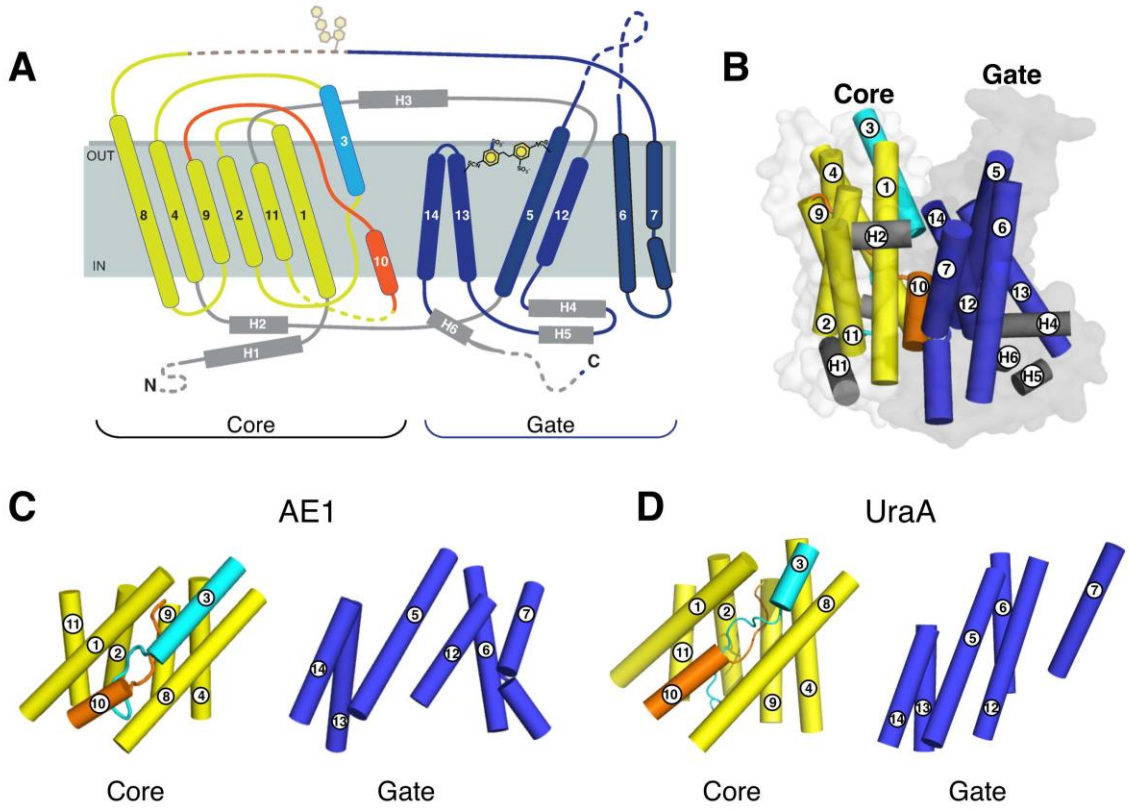

Fig. 2. Structural framework of AE1$_{CTD}$ and comparison with UraA. (A) Topology and **(B)** overall structure of AE1$_{CTD}$ viewed in the plane of the membrane. TM3 is colored in cyan and TM10 in orange. The other transmembrane helices of the Core domain are colored yellow and those of the Gate domain blue. **(C)** The Core and Gate domains of AE1. Left: the Core domain viewed from the Gate domain. Right: the Gate domain viewed from the Core domain. Coloring as in (A). **(D)** As (C) but for UraA, (PDB accession code 3QE7). The two proteins were aligned on their respective Core domains.

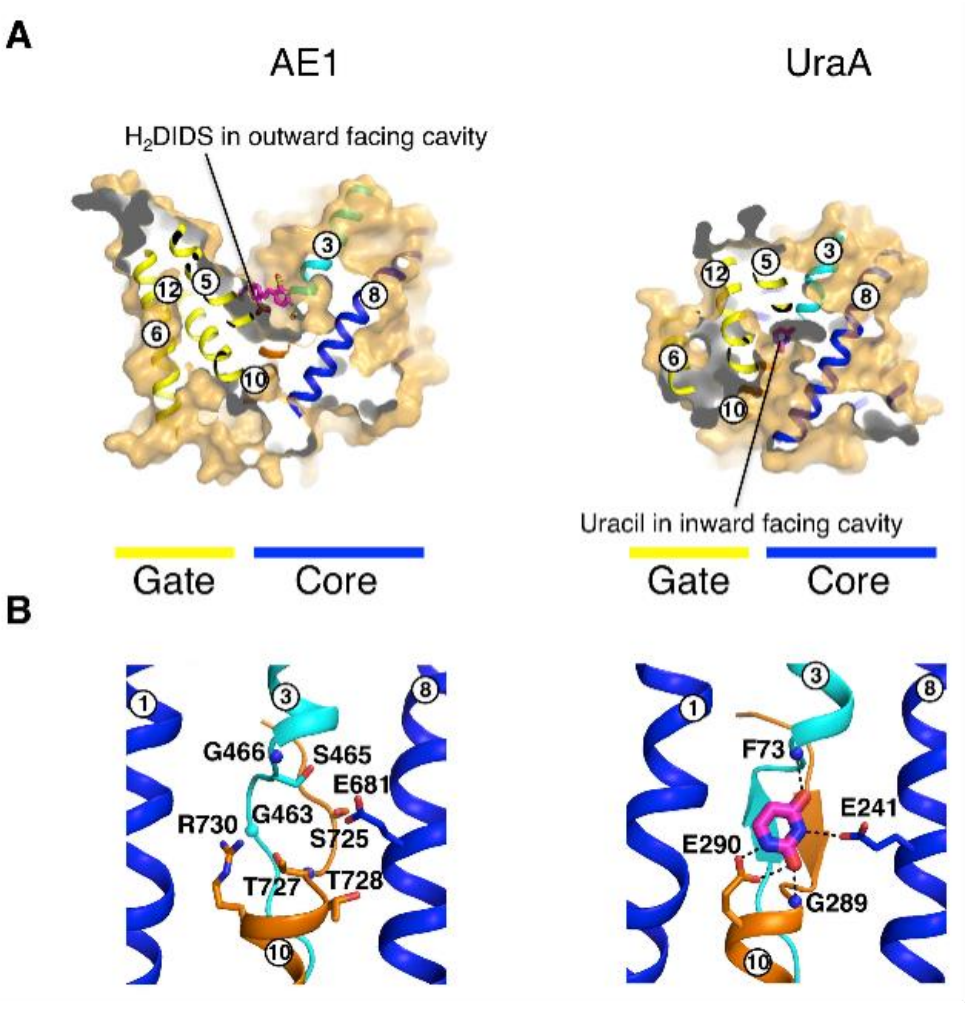

Fig. 3. Outward- and inward-facing cavities and substrate binding sites in AE1 and UraA. **(A)** Surface representations of the outward-facing structures of the substrate-free $AE1_{CTD}$ complex with H_2DIDS (left) and the inward-facing structure of UraA (PDB accession code 3QE7) with uracil (right). These are the views in the plane of the membrane. The surfaces are semi-transparent and slabbed to show the positions of the transmembrane helices, which are colored as in Fig. 2. The H_2DIDS and uracil are shown in magenta on the left and right panels, respectively. **(B)** Comparison of the putative anion binding site in AE1 (left) with the Uracil binding site in UraA (right). The coloring is as in (A). Glu241 and Glu290 of Uracil correspond to Glu681 and Arg730 of AE1 respectively. The dark blue spheres represent the amide nitrogens of the depicted residues and the light blue sphere the Cα atom of Gly463.

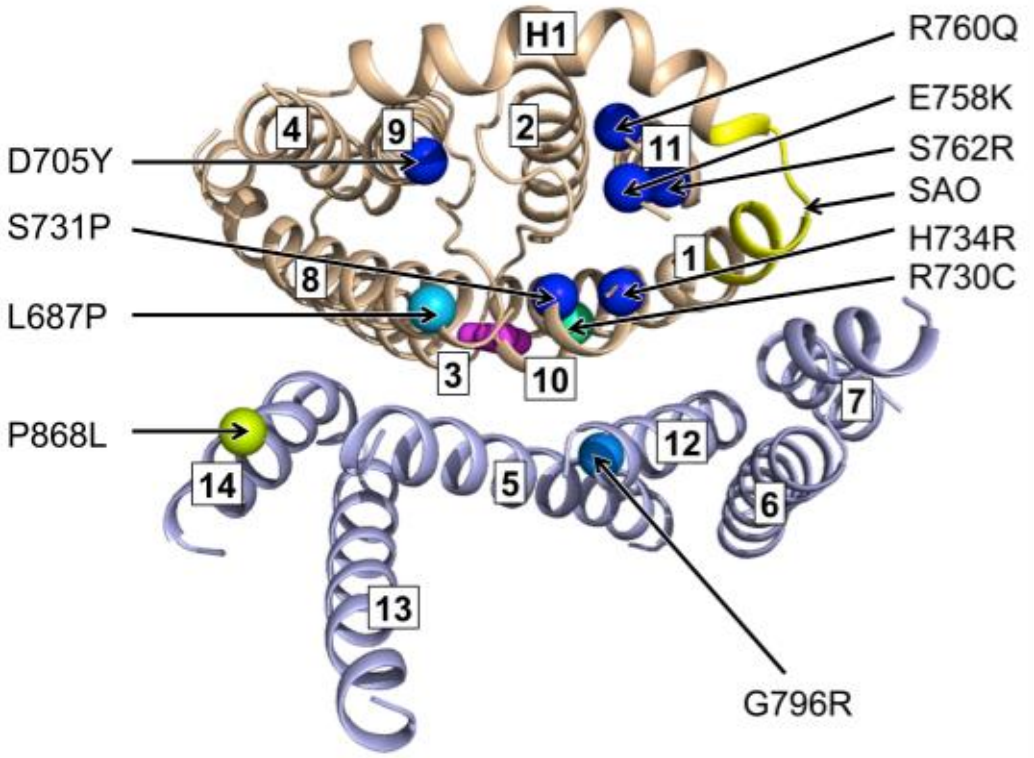

Fig. 4. Some mutations reported to cause diseases, plotted on the structure of $AE1_{CTD}$. The Core domain is colored coral and the Gate domain light blue. The view is from the cytoplasmic side of the membrane. The deletion mutation of residues 400-408, which causes SAO is shown in yellow. Point mutations are shown by spheres with coloring according to conservation among the 10 human SLC4 family transporters. This was generated with the ConSurf server (http://consurf.tau.ac.il/) (62) using AE1-4, NBCe1-2, NBCn1, NDCBE, NCBE and BTR1 and colored according to the colours of the rainbow with blue, highly conserved and red, poorly conserved. R730 is only conserved amongst the electrogenic family members. The details of mutations are described in Table S3 and Figs. S11 and S12. The position of uracil in the UraA structure, corresponding to the possible anion binding site in AE1, is shown with magenta spheres.